Journal of Molecular Catalysis B: Enzymatic 56 (2009) 300–306

Contents lists available at ScienceDirect

Journal of Molecular Catalysis B: Enzymatic

journal homepage: www.elsevier.com/locate/molcatb

Kinetic and thermodynamic characterization of the cold activity acquired upon single amino-acid substitution near the active site of a thermostable α-glucosidase

Akio Noguchi, Tokuzo Nishino, Toru Nakayama*

Department of Biomolecular Engineering, Graduate School of Engineering, Tohoku University, Aobayama 6-6-11, Aoba-ku, Sendai, Miyagi 980-8579, Japan

ARTICLE INFO

Article history:
Received 17 April 2008
Received in revised form 29 May 2008
Accepted 1 June 2008
Available online 17 June 2008

Keywords:
α-Glucosidase
Temperature dependence
Cold activity
Activation enthalpy
Optimum temperature
Thermostability
Psychrophilic enzymes
Flexibility

ABSTRACT

The α-glucosidase of *Bacillus* sp. SAM1606, a thermophilic bacterium, is a thermostable enzyme that has maximal activity at an apparent optimal temperature between 65 and 70 °C and only very low activity at low temperatures (0–25 °C). In this study, we identified Thr272, which is located adjacent to Glu271 (a catalytic residue) and Gly273 (a determinant of specificity), as a determinant of the optimal temperature, as substitution of Thr272 with other residues significantly altered the temperature–activity profile of the enzyme. Substitution of Thr272 with other amino acids, in particular bulky hydrophobic residues such as valine, methionine and phenylalanine, resulted in a significant downward shift (by 30 °C) of the apparent optimal temperature with an increase in catalytic activity at low temperatures. The observed downward shift of the apparent optimal temperature was not due to instability of the mutants at 40–65 °C, as the mutants were stable at temperatures up to 65 °C. Among the mutants examined, T272V displayed the highest k_{cat} values at 10–25 °C, which was at least 11-fold greater than the k_{cat} value observed for the wild-type enzyme. The thermodynamic characteristics of reactions catalyzed by T272V, T272M, T272F, and wild type at 25 °C were examined in greater detail. The T272V, T272M and T272F mutants displayed large K_s (or K_m) values and reduced $\Delta H^{\#}_{ES}$ and $\Delta S^{\#}_{ES}$ values at 25 °C, consistent with the general features of cold adaptation. The observed cold activities of T272V, T272M and T272F most likely arose from local flexibility of the active site at low temperatures due to loss of a Thr272-mediated hydrogen bond. However, this hydrogen-bond loss likely permits reversible conformational changes of the active site to less active forms at elevated temperatures (e.g., 60 °C). This may explain why catalytic activities for T272V, T272M and T272F at high temperatures (e.g., 60 °C) were lower than those at low temperature (e.g., 25 °C), even though the mutant enzymes appeared stable at 60 °C.

1. Introduction

The temperature–activity profile is an important characteristic of enzymatic reactions. Cold-adapted enzymes display higher molecular activities at low temperatures (i.e., cold activities) than their thermophilic counterparts [1]. The optimal temperatures of these psychrophilic enzymes are generally lower than those of thermophiles, mostly because psychrophilic enzymes are unstable at high temperatures. The cold activity and thermolability of psychrophilic enzymes may be the key to the successful use of these enzymes in some applications, including use as catalysts in organic syntheses of unstable compounds at low temperatures [2,3]. An inverse relationship between cold activity and thermostability also holds for thermostable enzymes, which display high stability at high temperatures and only very low cold activity. Thus, cold activity is often associated with thermolability. It has been hypothesized that both cold activity and thermolability arise from enzymatic structural flexibility [4]. Comparative crystallographic, biochemical, and biophysical studies of cold-adapted enzymes and their counterparts have shown that many cold-adapted enzymes display local flexibility, especially in regions adjacent to the active site [5,6]. Reactions catalyzed by cold-adapted enzymes are generally characterized by smaller changes in activation enthalpy ($\Delta H^{\#}$) as well as high k_{cat} and K_m (or K_s) values [5–7]. Moreover, it has been observed that the difference in the activation entropy change between reactions catalyzed by psychrophilic and mesophilic enzymes, $\Delta(\Delta S^{\#})$, is always negative [5–7]. So far, attempts have been made to improve the thermostability of cold-active enzymes without deteriorating catalytic efficiency at low temperatures [3,8].

* Corresponding author. Tel.: +81 22 795 7270; fax: +81 22 795 7270.
E-mail address: nakayama@seika.che.tohoku.ac.jp (T. Nakayama).

1381-1177/$ – see front matter © 2008 Elsevier B.V. All rights reserved.
doi:10.1016/j.molcatb.2008.06.006

α-Glucosidase (EC 3.2.1.20) catalyzes the hydrolysis of 1-*O*-α-D-glucopyranosides with a net retention of the anomeric configuration. The α-glucosidase from *Bacillus* sp. strain SAM1606, a thermophilic bacterium that preferentially grows at 60–65 °C [9], is a member of family 13 of the glycoside hydrolases with broad substrate specificity and the capacity to hydrolyze α,α′-trehalose [10,11]. The SAM1606 α-glucosidase is a thermostable enzyme (stable up to 70 °C for 10 min) that displays virtually no activity at temperatures less than 10 °C. To date, we have created 40 site-directed mutants, in which amino-acid residue(s) near the active site were replaced with other residue(s), based on mutational analyses of substrate specificity of this enzyme [11–15]. We found that two of these mutants, both of which contained an amino-acid substitution at position 272, showed temperature profiles that were significantly different from that of the wild-type enzyme, implying that the nature of the amino-acid residue at position 272 might affect the temperature–activity profile of the enzyme. Position 272 is located in the active-site pocket of the enzyme and adjacent to Glu271 (one of the catalytic residues of the enzyme) [10] and to Gly273, which governs enzyme specificity [11–15].

In this study, substitution mutants of α-glucosidase at position 272 were created using all other amino-acid residues (collectively termed T272X, where X represents the one-letter notation of the amino acid located at position 272) and the temperature–activity profiles of the mutants were determined. The apparent optimal temperature for many of these mutants was significantly less than (by 10–30 °C) that of the wild-type enzyme with an increase in cold activity. It is very interesting that these mutants appeared as thermostable as the wild type. The kinetic and thermodynamic behaviors of enzymatic α,α′-trehalose hydrolysis catalyzed by representative mutants (i.e., T272V, T272M, and T272F) were characterized. Mechanistic aspects of the results obtained were discussed with structural models of active sites of enzymes.

2. Materials and methods

2.1. Materials

α,α′-Trehalose was obtained from Merck KGaA, Darmstadt, Germany. *p*-Nitrophenyl-α-D-glucopyranoside (*p*NP-Glc) was obtained from Nacalai Tesque, Kyoto, Japan. All other chemicals were of analytical grade.

2.2. Bacterial stain and plasmids

The plasmid pGBSU5 [11] was used as a template for site-directed mutagenesis in preparation of T272X mutants. The plasmid pET-15b (Novagen, Madison, WI, U.S.A.) was used to express the wild-type and mutant α-glucosidase genes in *Escherichia coli* BL21 (DE3).

2.3. Site-directed mutagenesis, expression, and purification of wild-type and mutant α-glucosidases

The genes encoding T272X mutants of SAM1606 α-glucosidase were constructed via site-directed mutagenesis in the plasmid pGBSU5 [11] using a QuikChange™ Site-Directed Mutagenesis Kit (Stratagene, La Jolla, CA, U.S.A.) with synthetic oligonucleotide primers containing the desired mutation (not shown). Individual mutations were verified by DNA sequencing using a dye-terminator cycle-sequencing kit with a CEQ 2000 DNA analysis system (Beckman Coulter, Fullerton, CA, U.S.A.). A DNA fragment (619 bp in length) containing the mutated site was recovered after digestion of the plasmid with the restriction enzyme, SacII. This fragment was then substituted for the corresponding DNA sequence in pGBSU5 to obtain pGBAGX2.

The full-length, wild-type SAM1606 α-glucosidase gene was amplified by PCR using a template plasmid, pGBSU5, and PCR primers containing restriction enzyme sites (NdeI and BamHI). The PCR product was digested using NdeI and BamHI, and the resulting fragment was inserted into the NdeI and BamHI sites of pET-15b to obtain pET-h-BAG. The T272X genes in the pGBAGX2 plasmids (see above) were digested using BseRI, and this fragment was then inserted into the BseRI sites of pET-h-BAG to obtain pET-h-BAGX (X represents the one-letter notation for the amino acid located at position 272).

E. coli BL21 (DE3) cells carrying either the plasmid pET-h-BAG or pET-h-BAGX were grown at 37 °C in Luria-Bertani broth containing 50 μg/ml ampicillin until the OD_{600} reached 0.5–0.7. Isopropyl β-thiogalactoside was then added to a final concentration of 1 mM, followed by cultivation for an additional 4 h at 37 °C. Cells were collected by centrifugation (20 min, 3000 × *g*), suspended in 0.02 M potassium phosphate buffer (pH 7.4) containing 0.5 M NaCl (termed buffer A), disrupted at 4 °C by 10 cycles of ultrasonication (where one cycle corresponds to 20 kHz for 30 s followed by an interval of 1 min), and subjected to centrifugation (15,000 × *g*, 15 min). Polyethyleneimine was added to the resulting supernatant at a final concentration of 0.12%, and the mixture was allowed to stand at 4 °C for 30 min. After centrifugation, the supernatant was heated at 60 °C for 30 min, followed by centrifugation. The resulting enzyme solutions were used in preliminary analyses of temperature–activity profiles of enzymes using α,α′-trehalose as the substrate (see Sections 2.4 and 3.1 and Supplementary Fig. 1). For purification of the wild type, T272V, T272M, and T272F, the enzyme solution obtained from the crude extract of *E. coli* cells, harboring pET-h-BAG (for the wild type) or pET-h-BAGX (for T272V, T272M, or T272F), was applied to a His-Trap™ column (1 ml; GE Healthcare UK, Buckinghamshire, UK) that had been equilibrated with buffer A. The column was washed with 10 ml of buffer A containing 60 mM imidazole, followed by elution of the enzyme with 5 ml of buffer A containing 100 mM imidazole. The enzyme was dialyzed against 0.01 M potassium phosphate buffer (pH 7.2) at 4 °C overnight, and concentrated by ultrafiltration. Sodium dodecyl sulfate (SDS) polyacrylamide gel electrophoresis (PAGE) (acrylamide concentration, 10%) was performed as described by Laemmli [16]. Protein was stained with either silver stain or Coomassie Brilliant Blue R250, and then destained in a destaining solution (a 2:1:7 mixture of methanol, acetic acid, and water).

2.4. Enzyme assays

2.4.1. Method I

Enzymatic hydrolysis of *p*NP-Glc was monitored according to the amount of *p*-nitrophenol released at 20 and 55 °C. The standard assay mixture contained 3.0 μmol of *p*NP-Glc, 30 μmol of potassium phosphate buffer (pH 7.2), and the enzyme, in a final volume of 3.0 ml. The mixture without the enzyme was brought to the specified temperature. The reaction was started by addition of the enzyme, and then changes in absorbance at 405 nm were recorded using a spectrophotometer (Hitachi UV-2000) equipped with a temperature-controlled cell holder. The extinction coefficient for *p*-nitrophenol under these conditions was 13,400 cm^{-1} M^{-1} [9].

2.4.2. Method II

For kinetic analysis of hydrolysis of α,α′-trehalose, the reaction mixture contained varying amounts of α,α′-trehalose, 5 μmol of potassium phosphate buffer (pH 7.2) and the enzyme in a final volume of 500 μl. The substrate concentrations used for kinetic studies generally ranged from 0.2 to 5 K_m. The mixture without the enzyme

was brought to a temperature in the range of either 25–80 °C (for the wild type) or 10–75 °C (for T272X mutants). The reaction was started by addition of enzyme. After a 10-min incubation period, the reaction was stopped by addition of 50 μl of 1 M HCl, followed by incubation of the mixture at 30 °C for 1 h to ensure enzyme inactivation. The blank did not contain the enzyme. To a 100-μl portion of the mixture, 690 μl of 1 M potassium phosphate buffer (pH 7.2), 50 μl of 1 mg/ml glucose oxidase (from *Aspergillus niger*, Nacalai Tesque, Kyoto, Japan), 60 μl of 10 mM 4-aminoantipyrine, 50 μl of 20 mM 2,4-dichlorophenol, and 150 μl of 0.01 mg/ml horseradish peroxidase were added, in that order, and the resulting reaction mixture was incubated at 30 °C for 30 min. The amount of glucose in the mixture was determined from the increase in absorbance at 505 nm. One unit of enzyme is defined as the amount of enzyme that catalyzes the hydrolysis of 1 μmol of substrate per minute. K_m and V_{max} values, and their standard errors, were estimated by fitting the initial velocity data to the Michaelis–Menten equation using non-linear regression [17]. The absorption coefficient of purified SAM1606 α-glucosidase and its mutants, $A_{280,1\%}$ of 25.5, which was calculated from the amino-acid sequence, was used for unit calculations.

2.4.3. Method III

For determination of dissociation constants (K_s) of the enzyme–substrate (ES) complex in the presence of α,α′-trehalose, which is a competitive inhibitor, the reaction mixture contained varying amounts (0.003–3.0 μmol) of *p*NP-Glc, 6.0 μmol of α,α′-trehalose, 3.0 μmol of potassium phosphate buffer (pH 7.2), and the enzyme, in a final volume of 300 μl. The mixture without the enzyme was brought to 25 °C. The reaction was started by addition of the enzyme. After a 10-min incubation period, the reaction was stopped by the addition of 40 μl of 1 M HCl. The blank did not contain the enzyme. The pH of the mixture was increased to 9.2 by addition of 1.0 ml of a 1 M Tris–HCl buffer (pH 9.5). The amount of *p*-nitrophenol that was released into the mixture was determined from the increase in absorbance at 405 nm using the extinction coefficient for *p*-nitrophenol at pH 9.2—15,600 $cm^{-1}\,M^{-1}$. K_m and V_{max} values and their standard errors were estimated by fitting the initial velocity data to the Michaelis–Menten equation using non-linear regression [17]. K_s values were calculated from the following equation:

$$v = \frac{V_{max}[S]}{K_m\,(1 + [I]/K_s) + [S]} \tag{1}$$

where [S] and [I] denote concentrations of *p*NP-Glc and α,α′-trehalose (20 mM), respectively. Dissociation constants (K_P) of the enzyme–product (EP) complex with α-D-glucose, which is also a competitive inhibitor, were also determined for T272V and wild type, essentially as described above.

2.5. Stability studies

For the thermal stability studies, the enzyme was incubated in 10 mM potassium phosphate buffer (pH 7.2) at either 30, 40, 50, 60, 65, 70, or 80 °C. After a 10-min incubation period, aliquots were withdrawn and placed into tubes on ice, and assayed for remaining enzymatic activity as described above (method I).

2.6. Thermodynamic analyses

Enzymatic reactions can be described by the transition state theory, which assumes the existence of an activated complex $(ES)^{\#}$ in equilibrium with the ground-state ES complex [7]:

$$E + S \rightleftarrows ES \rightleftarrows (ES)^{\#} \rightarrow EP \rightleftarrows E + P \tag{2}$$

(see also Fig. 3). Thus, Gibbs free energy changes associated with formation of the ES (ΔG_+) and EP (ΔG_-) complexes, Gibbs free energy changes of activation ($\Delta G^{\#}_{ES}$), and the total Gibbs free energy changes of activation ($\Delta G^{\#}_{E+S}$) were calculated from the following equations:

$$\Delta G_+ = -RT \ln\left(\frac{1}{K_s}\right) \tag{3}$$

$$\Delta G_- = -RT \ln\left(\frac{1}{K_P}\right) \tag{4}$$

$$\Delta G^{\#}_{ES} = RT\left(\ln\left[\frac{k_B T}{h}\right] - \ln k_{cat}\right) \tag{5}$$

$$\Delta G^{\#}_{E+S} = \Delta G_+ + \Delta G^{\#}_{ES} \tag{6}$$

where k_B is the Boltzmann constant ($1.38 \times 10^{-23}\,J\,K^{-1}$), h is the Planck constant ($6.63 \times 10^{-34}\,J\,s$), R is the gas constant ($8.31\,J\,mol^{-1}\,K^{-1}$), and T is the temperature in Kelvin degrees.

Activation enthalpy changes, $\Delta H^{\#}_{ES}$, were obtained from the following equation:

$$\Delta H^{\#}_{ES} = \Delta E_a - RT \tag{7}$$

where ΔE_a is the activation energy determined from Arrhenius plots [7]. Activation entropy changes, $\Delta S^{\#}_{ES}$, were obtained from the following equation:

$$\Delta S^{\#}_{ES} = \frac{(\Delta H^{\#}_{ES} - \Delta G^{\#}_{ES})}{T} \tag{8}$$

$\Delta(\Delta G^{\#}_{ES})_{V-T}$, for example, denotes $\Delta G^{\#}_{ES}$ of T272V minus $\Delta G^{\#}_{ES}$ of the wild type (see Fig. 3).

3. Results and discussion

3.1. Temperature–activity profiles of α-glucosidase mutants

Previously, we created forty site-directed mutants of SAM1606 α-glucosidase [11–15] that have amino-acid substitution(s) near the active site. We initially expected that some of these substitutions might alter the environment of the active site, thereby affecting the temperature–activity profiles. Thus, we compared the catalytic activity of the mutants for *p*NP-Glc hydrolysis (final concentration, 1 mM; see Section 2.4; method I) at two different temperatures (20 and 55 °C), and the ratio of activity at 20 °C to activity at 55 °C, termed the $R_{20/55}$ value, was compared among mutants. The wild-type enzyme had an $R_{20/55}$ value of 0.09. Among the mutant enzymes examined, T272V and T272M displayed an exceptionally high $R_{20/55}$ value (1.0). Both of these mutants have an amino-acid substitution at position 272 in their primary structures, suggesting that the amino-acid residue at this position might affect the temperature–activity profiles of the enzyme. To examine this hypothesis in greater detail, the amino-acid residue at position 272 was replaced by 17 other amino acids. Each of the resulting mutants (collectively termed T272X) and the wild type were expressed as His_6-tagged fusions in *E. coli* cells and were partially purified. All mutants, except for T272R, were catalytically active. The temperature dependence of enzymatic activity of these mutants was analyzed using α,α′-trehalose (final concentration, 10 mM; see Section 2.4, method II) as the substrate. Relative %activity at assay temperature T, ($v_{rel,T}$), was plotted as a function of T, where $v_{rel,T}$ at the optimal temperature was taken to be 100% (Supplementary Fig. 1S).

Substitution of the amino acid at position 272 with either alanine, serine, or cysteine, which share a side chain that is similar in size or nature to that of threonine, did not significantly alter the temperature–activity profiles of the enzyme (Supplementary Fig.

1S(A)), showing an apparent optimal temperature at approximately 60 °C. Substitution with other amino acids (except for arginine) resulted in a downward shift of the apparent optimal temperature of the enzyme. Moreover, relative %activities of these mutants at 0 °C ($v_{rel,0}$) were greater than that of the wild-type enzyme. Substitution with hydrophobic amino acids, such as valine, methionine, and phenylalanine (Supplementary Fig. 1S (B, C)), generally resulted in higher $v_{rel,0}$ values and/or a lower shift of optimal temperatures than substitution with anionic amino acids (aspartic and glutamic acids; Supplementary Fig. 1S (D)), amide-containing amino acids or small amino acids (proline and glycine; Supplementary Fig. 1S (E)). Thus, we selected T272V, T272M and T272F for comparison of kinetic properties (Section 3.2), thermostabilities (Section 3.3), and thermodynamic properties (Section 3.4) with those of wild type. It must be mentioned that, because temperature–activity profiles of *p*NP-Glc hydrolysis catalyzed by these mutants were very similar to those of α,α′-trehalose hydrolysis (not shown), the observed alterations in temperature–activity profiles did not arise from changes in the substrate specificity of these mutants.

3.2. Temperature-dependent kinetic studies

To determine if the selected mutants (T272V, T272M and T272F) displayed greater cold activity than that of the wild type as a result of amino-acid substitution, these three mutants were purified to homogeneity based on SDS-PAGE, and temperature-dependent kinetic analyses of α,α′-trehalose hydrolysis catalyzed by the mutants were carried out. At 25 °C, these three mutants displayed higher k_{cat} values than that of the wild type (Fig. 1, see also Table 1). In particular, T272V displayed the highest k_{cat} value at 25 °C, which was 11-fold greater than the k_{cat} value observed for the wild type (Fig. 1A, inset). Thus, in terms of k_{cat} value, T272V, T272M and T272F exhibited greater "cold activity" than the wild-type enzyme. Substitution with these bulky hydrophobic amino acids at position 272 increased the K_m for trehalose at 25 °C (see also Table 1). As the temperature was increased to 35–40 °C, k_{cat} values for the T272V, T272M and T272F mutants increased without large changes in K_m values. At temperatures greater than 40 °C, the k_{cat} values decreased and the K_m values increased (Fig. 1). The apparent maximal k_{cat} and k_{cat}/K_m values for T272V, T272M and T272F were obtained at 30–40 °C and were less than the k_{cat} and k_{cat}/K_m values for the wild-type enzyme at 60 °C.

3.3. Stability studies

The downward shift in optimal temperature observed for T272V, T272M and T272F (see above) suggests that these amino-acid substitutions might render the enzyme unstable at high temperatures. For example, the optimal temperature for T272V was approximately 40 °C (Fig. 1), indicating that the mutants might be unstable at temperatures greater than 40 °C due to thermal inactivation of the mutants. However, stability studies showed that these three mutants were stable at temperatures as high as 65 °C under the assay conditions used in this study (Fig. 2). For comparison, the wild-type enzyme was stable up to 70 °C under the same conditions. These results suggest that the observed decrease in catalytic activity of the T272V, T272M and T272F mutants at 40–65 °C was most likely due to reversible, temperature-dependent conformational changes to less active forms (see also Section 3.5).

3.4. Thermodynamic analyses

To gain insight into the mechanism by which cold activity is acquired as a result of amino-acid substitution at position 272, we

Table 1
Kinetic and thermodynamic parameters of the wild-type SAM1606 α-glucosidase and its mutants (T272V, T272M, and T272F)[a]

Enzyme	k_{cat} (s^{-1})	K_m (mM)	k_{cat}/K_m (s^{-1} mM^{-1})	K_S (mM)	ΔG_+ (kJ mol^{-1})	$\Delta G^{\#}_{ES}$ (kJ mol^{-1})	$\Delta H^{\#}_{ES}$ (kJ mol^{-1})	$\Delta S^{\#}_{ES}$ (J mol^{-1} K^{-1})	$\Delta G^{\#}_{E+S}$ (kJ mol^{-1})	$\Delta(\Delta G_+)_{\chi-T}$[a] (kJ mol^{-1})	$\Delta(\Delta G^{\#}_{ES})_{\chi-T}$[a] (kJ mol^{-1})	$\Delta(\Delta G^{\#}_{E+S})_{\chi-T}$[a] (kJ mol^{-1})
At 25 °C												
Wild-type	0.30	2.2	0.14	3.9	−13.8	75.9	99.0	78	62.1	0	0	0
T272V	3.4	9.1	0.37	32	−8.6	70.0	34.5	−119	61.4	5.2	−5.9	−0.7
T272M	2.0	11	0.17	41	−7.9	71.3	55.9	−52	63.4	5.9	−4.6	1.3
T272F	2.6	7.7	0.34	6.9	−12.3	70.6	78.4	26	58.3	1.5	−5.3	−3.8
At 60 °C												
Wild-type	43	9.0	4.8	11	−12.6	71.5	98.7	82	58.9	0	0	0
T272V	3.8	17	0.22	17	−11.3	78.2	34.2	−132	66.8	−1.3	6.7	7.9

[a] Kinetic and thermodynamic parameters were determined as described in Sections 2.4 and 2.6, respectively. $\Delta(\Delta G_+)_{\chi-T}$, for example, denotes ΔG_+ of T272V minus ΔG_+ of the wild type.

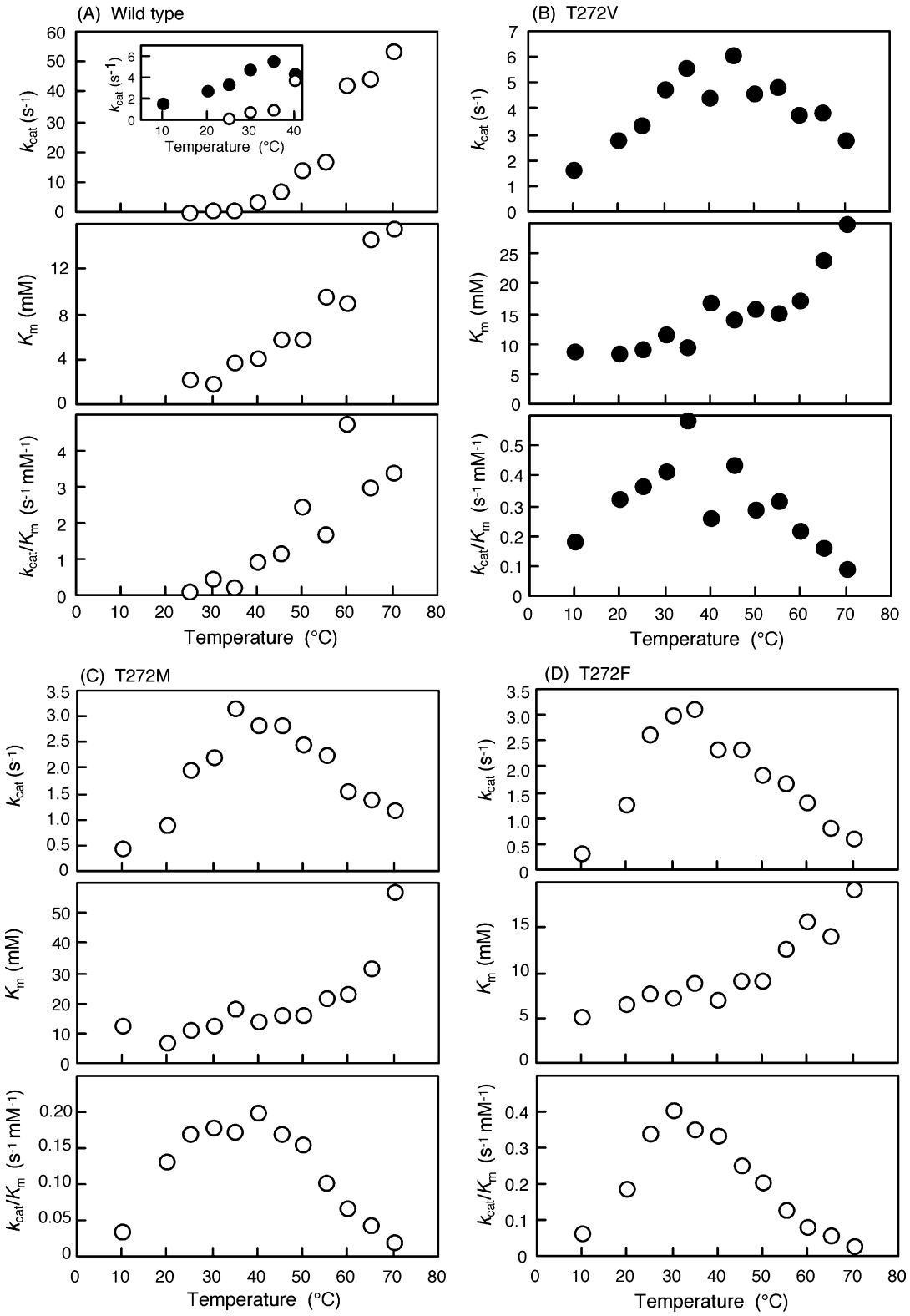

Fig. 1. Temperature dependences of kinetic parameters of hydrolysis of α,α′-trehalose catalyzed by wild-type SAM1606 α-glucosidase (A) and its mutants (B, T272V; C, T272M; and D, T272F). Inset in panel (A) shows a comparison of k_{cat} values of wild-type enzyme (open circles) and mutant T272V (closed circles) at temperatures less than 40 °C. Experimental conditions are described in Section 2.4 (method II). Standard errors of k_{cat} and K_m values were generally within ±20% and ±30%, respectively.

analyzed the thermodynamic parameters of α,α′-trehalose hydrolysis catalyzed by selected mutants (see above) and the wild-type enzyme at 25 °C (Fig. 3, see also Table 1). The wild-type enzyme displayed very low, but measurable, activity at 25 °C. Linear relationships in the Arrhenius plots of T272V, T272M, T272F, and the wild type were observed at temperatures less than 40 °C (not shown), allowing us to estimate the activation energies (ΔE_a) for reactions catalyzed at 25 °C. K_s and K_p values were also determined

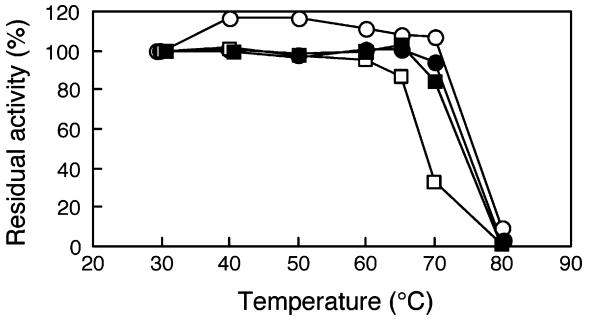

Fig. 2. Thermostabilities of wild-type enzyme (open circles), T272V (closed circles), T272M (open squares), and T272F (closed squares) mutants. For experimental details, see Section 2.5.

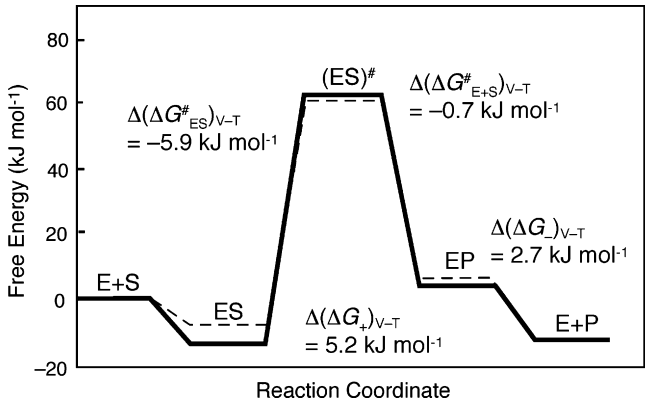

Fig. 3. Energy-level diagrams (according to Eq. (2)) of α,α′-trehalose hydrolysis catalyzed by the wild-type enzyme (thick lines) and the T272V mutant (dotted lines) at 25 °C. Values were calculated from the kinetic parameters shown in Table 1 using Eqs. (3)–(6). The symbols "E + S", "ES", "(ES)#″", "EP", and "E + P" represent the free enzyme plus substrate, the Michaelis enzyme–substrate complex, the activated complex, the Michaelis enzyme–product complex, and the free enzyme plus product, respectively. The energy levels of the (E + S) state of enzymes were taken to be 0 kJ mol^{-1}. $\Delta(\Delta G^{\#}_{ES})_{V-T}$, for example, denotes $\Delta G^{\#}_{ES}$ of T272V minus $\Delta G^{\#}_{ES}$ of the wild type. The k_{cat} value of enzymatic reaction can be increased by stabilizing (ES)# or destabilizing ES.

at 25 °C to determine free energy changes (ΔG_+ and ΔG_-) for the formation of ES and the EP complexes from the (E + S) and the (E + P) states, respectively.

The activation free energy change, $\Delta G^{\#}_{E+S}$, from the (E + S) state to the transition state (ES)# of T272V-catalyzed reactions (61.4 kJ mol^{-1}) was only slightly decreased from that of the wild-type enzyme (62.1 kJ mol^{-1}) (Table 1, see also Fig. 3). In contrast, the calculated free energy changes (ΔG_+) for the formation of the ES complex from the (E + S) state suggested that the ES complex was destabilized by 5.2 kJ mol^{-1} in the T272V-catalyzed reaction as compared with the wild-type reaction (Fig. 3), reflecting a large decrease in affinity of the mutant enzyme for the substrate. As a result, $\Delta G^{\#}_{ES}$ of the T272V-catalyzed reaction (70.0 kJ mol^{-1}) was much less (by $\Delta(\Delta G^{\#}_{ES})_{V-T}$ of −5.9 kJ mol^{-1}) than that of the wild type (75.9 kJ mol^{-1}), resulting in a significant (11-fold) increase in the k_{cat} value of T272V at 25 °C (Fig. 3). The observed decrease in the $\Delta G^{\#}_{ES}$ value of T272V could be further resolved into two components—the $\Delta H^{\#}_{ES}$ and $\Delta S^{\#}_{ES}$ terms. The increase in k_{cat} at 25 °C as a result of the T272V substitution was attributed to a large decrease in $\Delta H^{\#}_{ES}$ (34.5 kJ mol^{-1} for T272V vs 99.0 kJ mol^{-1} for the wild type), accompanied by a large decrease in $\Delta S^{\#}_{ES}$ (−119 J mol^{-1} K^{-1}), which differed markedly from the wild-type enzyme ($\Delta S^{\#}_{ES}$, 78 J mol^{-1} K^{-1}) (Table 1). These features (i.e., large K_s (or K_m) values and reduced $\Delta H^{\#}_{ES}$ and $\Delta S^{\#}_{ES}$ values) were also observed for T272M and T272F mutants at 25 °C (Table 1) and were consistent with the general thermodynamic features of reactions catalyzed by cold-adapted enzymes [5–7] (see Section 1).

3.5. Structural and mechanistic considerations

The k_{cat} values of enzymatic reactions can be enhanced by decreasing $\Delta H^{\#}_{ES}$ and increasing $\Delta S^{\#}_{ES}$, and the former can be considered as the main adaptive characteristic of low temperatures [6,7]. The decrease in $\Delta H^{\#}_{ES}$ in reactions catalyzed by cold-adapted enzymes is related to the reduced number of enthalpy-related interactions (such as hydrogen bonds and electrostatic interactions) that have to be disrupted for formation of the transition state [6,7]. The reduced number of such interactions enhances flexibility of the ground-state ES complex; i.e., a greater number of possible conformational states (a high S_{ES} level); hence, the transition state has to be formed with a greater decrease in entropy. Thus, a decrease in $\Delta H^{\#}_{ES}$ is inherently accompanied by a decrease in $\Delta S^{\#}_{ES}$ for the

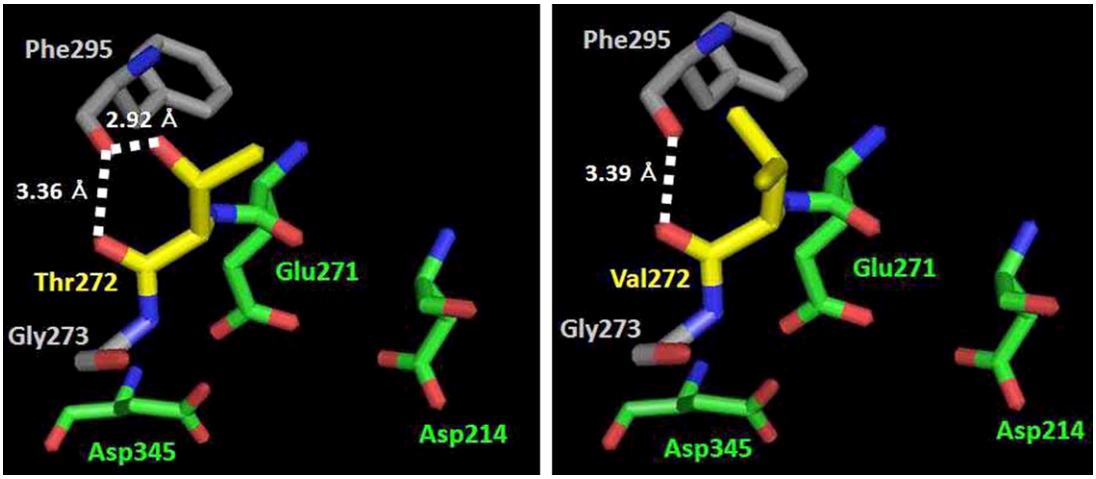

Fig. 4. Close-up view of the modeled active site of SAM1606 α-glucosidase (left panel) and its T272V mutant (right panel). Three-dimensional structures were built using coordinates from the X-ray structure of O16G of *B. cereus* ATCC7064 ([18]; PDB ID, 1UOK) as a template by means of SWISS-MODEL, which is accessible via the ExPASy web server (http://br.expasy.org/). Putative catalytic residues (Asp214, Glu271, and Asp345) are shown in green. Thr272 of the wild-type enzyme is shown in yellow. Dotted lines show predicted hydrogen bonds of Thr272 (left panel) or Val272 (right panel) with Phe295.

enzymatic reaction—the former increases the k_{cat} value, while the latter reduces the k_{cat} value. In reactions catalyzed by cold-adapted enzymes at low temperatures, the decrease in $\Delta H^{\#}_{ES}$ exceeds the decrease in $T\Delta S^{\#}_{ES}$, resulting in a net decrease in $\Delta G^{\#}_{ES}$ value and, therefore, an increase in the k_{cat} value.

Three-dimensional structural models of the wild-type enzyme and T272V were built with the coordinates from the X-ray structure of oligo-1,6-glucosidase of *B. cereus* ATCC7064 ([18], PDB ID 1UOK; sequence identity, 67%) as a template to explore the mechanism responsible for the acquired cold activity. Molecular modeling of the wild-type enzyme predicts that the 1-hydroxyethyl moiety of Thr272 is oriented towards the hydrophobic interior of the enzyme, is hydrogen-bonded with the main-chain oxygen atom of Phe295 (Fig. 4), and is in an ordered state. Exchange of the hydroxy group of Thr272 with a methyl group (i.e., T272V substitution) eliminates this hydrogen bond. The Val272 in the T272V mutant should occur in a less-ordered state than Thr272 in the wild-type enzyme. Because position 272 is located in close proximity to the catalytic site of the enzyme (Fig. 4), the active site of the ground-state ES complex of T272V might also be more flexible than that of the wild type. Thus, the observed increase in k_{cat} for T272V at 25 °C can be explained by enhanced local flexibility in the active site of the ES complex for T272V due to loss of the hydrogen bond. The observed $\Delta(\Delta H^{\#}_{ES})_{V-T}$ value (−64.5 kJ mol^{-1}) may be accompanied by a negative $\Delta(\Delta S^{\#}_{ES})_{V-T}$ value, −197 J mol^{-1} K^{-1}, producing an overall change in $\Delta(\Delta G^{\#}_{ES})_{V-T}$ of −5.9 kJ mol^{-1}. This decrease in $\Delta G^{\#}_{ES}$ approximately corresponded to the free energy change for destabilization of the ES complex of α-glucosidase ($\Delta(\Delta G_{+})_{V-T}$, 5.2 kJ mol^{-1}; see above).

The T272V mutant could be a cold-active enzyme with apparent stability at 60 °C, but catalytic activity of the mutant at 60 °C was significantly lower than the value expected from extrapolation of its cold activity. The observed decrease in k_{cat} values for T272V at 40–65 °C could likely arise from reversible, temperature-dependent conformational changes of the active site in the mutant at high temperatures to less active forms of the ground-state ES complex due to increased flexibility of the environment near the active site. The high activity and low stability of cold-adapted enzymes purportedly illustrate the general principle of activity–stability trade-off [6,7]. Although the local flexibility near the active site of the ES complex in this mutant did not appear to make the entire enzyme molecule unstable, it may allow local, reversible conformational changes around the active site at elevated temperatures (e.g., 60 °C), which result only in low k_{cat} values. Thus, in essence, this α-glucosidase is bound by the "activity–stability trade-off" principle. The hydrogen bond between Thr 272 and Phe295 may serve as a "molecular clasp" that prevents the reversible conformational change in the active site, thereby maintaining the enzyme in its most active form at elevated temperatures.

Molecular modeling also predicted that neither T272M nor T272F has a hydrogen bond between side chain of the amino acid at position 272 and Phe295. Both the T272M and T272F mutants consistently displayed k_{cat} values that were greater than the wild-type value (Table 1). The observed decrease in k_{cat} values for T272M and T272F at 40–65 °C could also arise from reversible, temperature-dependent conformational changes in these mutants at high temperatures, as in the case of T272V. The fact that the T272S and T272C mutants showed temperature–activity profiles that were very similar to that of the wild type could be consistently explained in terms of the possible formation of a hydrogen bond with Phe295 through the side chains of Ser272 and Cys272, respectively. It must be mentioned, however, that T272A displayed a temperature–activity profile that was similar to that of the wild type (see Supplementary Fig. 1S(A)), although T272A was predicted to be devoid of a hydrogen bond between the side chain of amino acid at position 272 and Phe295. To address this issue, we purified T272A to homogeneity and examined its kinetic properties at 25 °C and thermostability. The results showed that T272A was stable up to 70 °C under the conditions described in Section 3.3 and displayed k_{cat} (1.1 s^{-1}) and K_m (1.6 mM) values, which were 3.7- and 0.7-times as high as the respective values of the wild type. Thus, T272A displayed catalytic activity that was higher than the wild type at 25 °C, consistent with the absence of a hydrogen bond between the side chain of amino acid at position 272 and Phe295. Unlike T272V, however, T272A appears not to undergo the reversible conformational changes at high temperatures to less active forms. These results may illustrate the complex nature of structural changes induced upon mutation. Substitution of Thr272 by an amino acid that is significantly different in size and shape from threonine might affect the mobility of the active site of the enzyme in different manners. The possibilities of such unpredictable effects must be addressed through future studies.

Acknowledgment

We are grateful to Kazuhiro Ohara, Tohoku University, for his help with molecular modeling studies and fruitful discussion.

Appendix A. Supplementary data

Supplementary data associated with this article can be found, in the online version, at doi:10.1016/j.molcatb.2008.06.006.

References

[1] C. Gerday, M. Aittaleb, J.L. Arpigny, E. Baise, J.-P. Chessa, G. Garsoux, I. Petrescu, G. Feller, Biochim. Biophys. Acta 1342 (1997) 119–131.
[2] C. Gerday, M. Aittaleb, M. Bentahir, J.P. Chessa, P. Claverie, T. Collins, S. D'Amico, J. Dumont, G. Garsoux, D. Georlette, A. Hoyoux, T. Lonhienne, M.A. Meuwis, G. Feller, Trends Biotechnol. 18 (2000) 103–107.
[3] A. Galkin, L. Kulakova, T. Nakayama, T. Nishino, N. Esaki, in: M. Fingerman, R. Nagabhushanam (Eds.), Recent Advances in Marine Biotechnology, vol. 8, Science Publishers, Inc., Enfield, NH, USA, 2003, pp. 1–27.
[4] P.W. Hochachka, G.N. Somero, Temperature Adaptation in Biochemical Adaptation, Princeton University Press, Princeton, 1984, pp. 355–449.
[5] S. D'Amico, P. Claverie, T. Collins, D. Georlette, E. Gratia, A. Hoyoux, M.A. Meuwis, G. Feller, C. Gerday, Phil. Trans. R. Soc. Lond. B 357 (2002) 917–925.
[6] K.S. Siddiqui, R. Cavicchioli, Ann. Rev. Biochem. 75 (2006) 403–433.
[7] T. Lonhienne, C. Gerday, G. Feller, Biochim. Biophys. Acta 1543 (2000) 1–10.
[8] L. Kulakova, A. Galkin, T. Nakayama, T. Nishino, N. Esaki, J. Mol. Catal. B: Enzyme 22 (2003) 113–117.
[9] M. Nakao, T. Nakayama, M. Harada, A. Kakudo, H. Ikemoto, S. Kobayashi, Y. Shibano, Appl. Microbiol. Biotech. 41 (1994) 337–343.
[10] M. Nakao, T. Nakayama, A. Kakudo, M. Inohara, M. Harada, F. Omura, Y. Shibano, Eur. J. Biochem. 220 (1994) 293–300.
[11] M. Inohara-Ochiai, T. Nakayama, R. Goto, M. Nakao, T. Ueda, Y. Shibano, J. Biol. Chem. 272 (1997) 1601–1607.
[12] M. Inohara-Ochiai, M. Okada, T. Nakayama, H. Hemmi, T. Ueda, T. Iwashita, Y. Kan, Y. Shibano, T. Ashikari, T. Nishino, J. Biosci. Bioeng. 89 (2000) 431–437.
[13] M. Okada, T. Nakayama, A. Noguchi, M. Yano, H. Hemmi, T. Nishino, T. Ueda, J. Mol. Catal. B: Enzyme 16 (2002) 265–274.
[14] A. Noguchi, T. Nakayama, H. Hemmi, T. Nishino, Biochem. Biophys. Res. Commun. 304 (2003) 684–690.
[15] A. Noguchi, M. Yano, Y. Ohshima, H. Hemmi, M. Inohara-Ochiai, M. Okada, K.-S. Min, T. Nakayama, T. Nishino, J. Biochem. (Tokyo) 134 (2003) 543–550.
[16] U.K. Laemmli, Nature 227 (1970) 680–685.
[17] R.J. Leatherbarrow, Trends Biochem. Sci. 15 (1990) 455–458.
[18] K. Watanabe, Y. Hata, H. Kizaki, Y. Katsube, Y. Suzuki, J. Mol. Biol. 268 (1997) 142–153.